Heat conduction in carbon nanotube materials: Strong effect of intrinsic thermal conductivity of carbon nanotubes

Alexey N. Volkov[a] and Leonid V. Zhigilei[b]
Department of Materials Science and Engineering, University of Virginia, 395 McCormick Road, Charlottesville, Virginia 22904-4745, USA

(Received 22 January 2012; accepted 5 July 2012; published online 24 July 2012)

Computational study of thermal conductivity of interconnected networks of bundles in carbon nanotube (CNT) films reveals a strong effect of the finite thermal conductivity k_T of individual nanotubes on the conductivity k of the CNT materials. The physical origin of this effect is explained in a theoretical analysis of systems composed of straight randomly dispersed CNTs. An analytical equation for quantitative description of the effect of finite k_T on the value of k is obtained and adopted for continuous networks of bundles characteristic of CNT films and buckypaper. Contrary to the common assumption of the dominant effect of the contact conductance, the contribution of the finite k_T is found to control the value of k at material densities and CNT lengths typical for real materials. © *2012 American Institute of Physics*. [http://dx.doi.org/10.1063/1.4737903]

Experimental measurements of thermal conductivity of individual CNTs, k_T, reveal exceptionally high room temperature values ranging from 1400 $Wm^{-1}K^{-1}$ to 3000 $Wm^{-1}K^{-1}$ for multi-walled CNTs (Refs. 1–4) and even higher values for single-walled CNTs.[3,5] These values by far exceed the thermal conductivity characteristic of most of the conventional materials and suggest that CNTs are among the most promising structural elements for the design of new nanomaterials for heat management applications. The exceptionally high thermal conductivity of individual CNTs, however, does not translate into correspondingly high thermal conductivity, k, of CNT materials, such as CNT films, mats, buckypaper, and vertically aligned arrays, which exhibit fairly small thermal conductivity in the range[6–9] of 10–220 $Wm^{-1}K^{-1}$ and even down to ~0.1 $Wm^{-1}K^{-1}$.[10]

It is generally accepted that the thermal conductivity of CNT materials is limited by the weak thermal coupling between the individual CNTs (Refs. 10–17) rather that the heat conduction within individual CNTs. To evaluate the relative importance of thermal transport by intrinsic conductivity and contact conductance in a CNT material, one can calculate the equivalent length of a CNT segment, L_{eq}, which has the same thermal resistance as a single thermal contact.[12] This equivalent length can be found by equating the corresponding heat fluxes needed to support the same temperature difference ΔT across a CNT contact and along the CNT segment of length L_{eq}, $k_T A_T \Delta T / L_{eq} = \sigma_c \Delta T$, where L_T and A_T are the nanotube length and cross-sectional area and σ_c is the effective inter-tube contact conductance. For single-walled (10,10) CNTs taken as an example, the equivalent length can be evaluated by using $\sigma_c = 5 \times 10^{-11}$ W K^{-1} predicted in atomistic calculations for two (10,10) CNTs crossing each other at 90° angle,[10] and defining $A_T = 2\pi R_T \delta_T$, where $R_T = 6.785$ Å is the radius of a CNT and $\delta_T = 3.4$ Å is the interlayer spacing in graphite. For $k_T = 2000$ $Wm^{-1}K^{-1}$, the thermal resistance of an inter-tube contact is equivalent to the thermal resistance of a CNT segment with $L_{eq} = 59$ μm. At first sight, this estimation appears to support the notion of small or even negligible effect of the intrinsic thermal resistance of CNTs on the effective conductivity of a network material composed of CNTs. The assumption of negligible contribution of the intrinsic thermal resistance of CNTs and, therefore, constant temperature of individual CNTs, is indeed commonly used in theoretical models aimed at prediction of the effective thermal conductivity of CNT materials, e.g., Refs. 10, 17, and 18.

In this letter, the validity of this assumption is evaluated in a series of calculations of thermal conductivity of continuous networks of (10,10) CNT bundles generated in mesoscopic simulations and exhibiting structural characteristics typical of CNT films and buckypaper.[19,20] The intrinsic thermal resistance of CNTs is found to make the dominant contribution to the effective thermal resistance of the CNT material for any reasonable value of k_T and L_T exceeding several hundreds of nanometers. This unexpectedly strong effect of the large but finite values of k_T is confirmed in a theoretical analysis that provides the conductivity scaling law for samples composed of randomly dispersed straight CNTs. The extension of the scaling law to the networks of bundles is demonstrated through the introduction of a semi-empirical parameter characterizing the effective contact conductance in the continuous network structures.

The samples used in the calculations of thermal conductivity are generated with a mesoscopic model that represents individual CNTs as chains of stretchable cylindrical segments[21] and accounts for the internal stretching, bending, and buckling of nanotubes,[20,21] as well as for the van der Waals interactions among the CNTs.[19] The simulations performed for systems composed of randomly distributed and oriented CNTs predict spontaneous self-assembly of CNTs into continuous networks of bundles with partial hexagonal ordering of CNTs in the bundles and preferential orientation of the bundles parallel to the planes of the films.[19,20] The network structures produced in the simulations are stabilized by the presence of multiple bending buckling kinks[20] and are similar to the structures of CNT films observed in

[a]Electronic mail: av4h@virginia.edu.
[b]Author to whom correspondence should be addressed. Electronic mail: lz2n@virginia.edu.

experiments.[22–24] All simulations are performed for films consisting of (10,10) single-walled CNTs with length L_T varying from 100 nm to 1 μm. The films have thickness of 20 to 100 nm and density of 0.2 g cm^{-3}, typical for CNT films.[22]

The calculation of in-plane thermal conductivity k of the CNT films is performed with a method suggested in Ref. 17 and enhanced with treatment of finite thermal conductivity of the nanotubes. The thermal conductivity is calculated by connecting two sides of a static network structure generated in a mesoscopic simulation to two heat baths maintained at different temperatures and evaluating the steady-state heat flux Q_x and temperature gradient ∇T_x established in the sample. The thermal conductivity can then be found from the Fourier law, $k = -Q_x/(\nabla T_x A_x)$, where A_x is the cross-sectional area of the sample in the direction perpendicular to the applied temperature gradient (x-axis in Fig. 1).

The evaluation of Q_x requires determination of temperature distributions in all CNTs defined by contact and intrinsic heat fluxes. The contact heat flux between nanotubes is defined through the "heat transfer" function $\psi(r)$ that depends on the distance r between points on the surfaces of nanotubes.[17] For isothermal nanotubes ($k_T = \infty$), contact heat flux between nanotubes i and j, Q_{ij}, is calculated as $Q_{ij} = \sigma_{cij}(T_j - T_i)$, where the contact thermal conductance $\sigma_{cij} = \sigma_{c0}\Psi_{ij}/\Psi_0$ depends on geometrical arrangement of CNTs through function $\Psi_{ij} = n_\sigma^2 \int\int \psi(r) dS_i dS_j$, where the integration is performed over the surfaces of interacting nanotubes, n_σ is the number density of atoms on the nanotube surface, and σ_{c0} is the conductance for a particular geometrical arrangement of nanotubes when $\Psi_{ij} = \Psi_0$. In a case of non-isothermal CNTs (finite k_T), the heat flux between a part of CNT i extending from one end ($l_i = 0$) up to the length l and the whole CNT j can be expressed as $Q_{ij}(l) = (n_\sigma^2 \sigma_{c0}/\Psi_0) \int\int \psi(r)(T_j(l_j) - T_i(l_i)) dS_i dS_j$, where $T_i(l_i)$ is the distribution of temperature along the CNT length l_i ($0 \le l_i \le L_T$) and the integration is over the surface of a part of CNT i ($0 \le l_i \le l$) and the whole CNT j. The value of $\sigma_{c0} = 5 \times 10^{-11}$ W K^{-1} for two (10,10) CNTs crossing each other at 90° angle is chosen in this work based on the results of atomistic Green's function calculations.[10]

The temperature distribution along an individual nanotube i that belongs to a percolating cluster in a CNT network and does not cross the heat bath boundaries is determined from the heat conduction equation

$$\frac{d}{dl_i}\left(A_T k_T \frac{dT_i}{dl_i}\right) = -\sum_{j=1}^{N} \frac{dQ_{ij}(l_i)}{dl_i}, \quad (1)$$

solved with boundary conditions $dT_i/dl_i = 0$ at $l_i = 0$ and $l_i = L_T$. This equation accounts for both the internal heat conduction described by the Fourier law $Q_i = -k_T A_T dT_i/dl_i$, and the heat exchange with surrounding nanotubes. The solution of Eq. (1) for all CNTs in the system enclosed between the hot and cold heat baths yields the steady-state heat flux Q_x and enables evaluation of the thermal conductivity of the material. In the case of $k_T = \infty$, the calculation of temperatures of CNTs reduces to balancing of the contact heat fluxes in each CNT.

Since experimental measurements[1–5] and theoretical calculations[25–27] of thermal conductivity k_T of individual CNTs yield a broad range of values, the simulations reported in this work are performed with $k_T = 200$ Wm^{-1}K^{-1}, 600 Wm^{-1}K^{-1}, 2000 Wm^{-1}K^{-1}, and $k_T = \infty$. The simulations demonstrate that the temperature variations along individual CNTs at finite k_T remain fairly small (Fig. 1). This is not surprising since L_{eq} is large in all simulations, e.g., $L_{eq} = 5.9\,\mu$m at $k_T = 200$ Wm^{-1}K^{-1} and $L_{eq} = 59\,\mu$m at $k_T = 2000$ Wm^{-1}K^{-1}. Nevertheless, the thermal conductivity of the film is strongly reduced when the finite value of k_T is used in the calculations (Fig. 2). Even for a relatively high intrinsic conductivity $k_T = 2000$ Wm^{-1}K^{-1} and $L_T = 1\,\mu$m, the value of the effective conductivity of the CNT network is ~3.5 times smaller than that at $k_T = \infty$. For

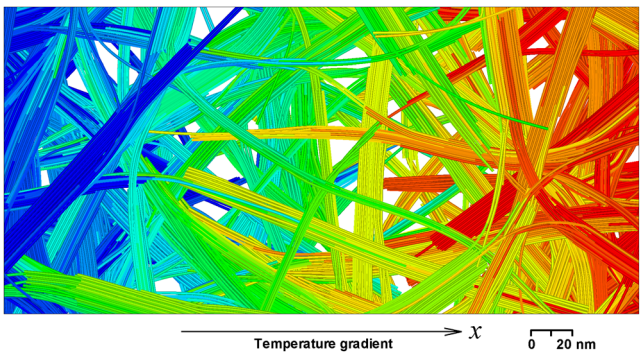

FIG. 1. A fragment of one of the CNT film structures generated in a mesoscopic simulation and used in the calculations of thermal conductivity k. The picture shows a part of a larger (500 nm × 500 nm × 100 nm) sample composed of (10,10) CNTs with $L_T = 200$ nm and material density of 0.2 g cm^{-3}. Left and right sides of the sample are connected with heat baths and temperature gradient is applied in the horizontal direction. Individual nanotubes are colored by their temperatures calculated with $k_T = 200$ W m^{-1} K^{-1}. Despite the relatively small conductivity of individual CNTs adopted in the simulation, the temperature variations along CNTs are fairly small and all nanotubes arranged into a bundle tend to maintain similar temperatures.

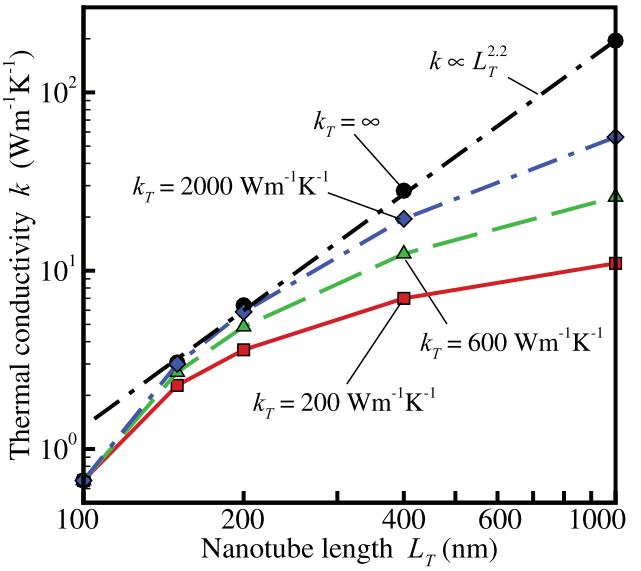

FIG. 2. Thermal conductivity k of CNT films generated in mesoscopic simulations vs. nanotube length L_T for $k_T = 200$ Wm^{-1}K^{-1} (squares), $k_T = 600$ Wm^{-1}K^{-1} (triangles), $k_T = 2000$ Wm^{-1}K^{-1} (diamonds), and $k_T = \infty$ (circles). Dash-double-dotted line is the power law $k \propto L_T^{2.2}$ fit to the values obtained at $k_T = \infty$ for $L_T \ge 150$ nm.

longer nanotubes, the relative contribution of the intrinsic thermal resistance of CNTs to the effective thermal resistance of the CNT material should increase, since the ratio k/k^0 (k^0 is the conductivity at $k_T = \infty$) decreases with increasing L_T/L_{eq}, as it is apparent from data in Fig. 2.

We believe that the strong reduction of the conductivity of the CNT films due to the finite thermal conductivity of individual nanotubes, revealed in the mesoscopic simulations, is not a peculiarity specific for the networks of interconnected CNT bundles, but a general trend common for network structures composed of conducting fibers. To support this claim, we perform a theoretical analysis of the relation between k and k^0 for two-dimensional (2D) and three-dimensional (3D) isotropic networks composed of randomly dispersed straight nanotubes. A soft-core approach[28,29] is used to define thermal contacts between nanotubes, i.e., the CNTs are allowed to intersect each other, and every intersection of a pair of CNTs is treated as a thermal contact with a constant contact conductance σ_c. This approach is similar to that used in Refs. 17 and 18 for systems with $k_T = \infty$, with the main difference being that distributions of temperature along the nanotubes are now calculated based on Eq. (1). For the soft-core CNTs with well-defined points of thermal contacts, the right-hand side of Eq. (1) reduces to $-\sum_{j=1,\delta_{ij}=1}^{N} \delta(l_i - l_{ij})\sigma_c(T_j(l_{ji}) - T_i(l_{ij}))$, where $\delta(l)$ is the Dirac δ-function, l_{ij} is the position of thermal contact between CNTs i and j on the axis of CNT i, and $\delta_{ij} = 1$ for CNT pairs that are in thermal contact with each other. Integration of Eq. (1) along the length of CNT i yields

$$\frac{T_i|_{l_i=L_T} - T_i|_{l_i=0}}{L_T\cos\theta_i} = \mathrm{Bi}_c \sum_{\substack{j=1 \\ \delta_{ij}=1}}^{N} \frac{T_j(l_{ji}) - T_i(l_{ij})}{L_T\cos\theta_i}\frac{l_{ij} - L_T}{L_T}, \quad (2)$$

where θ_i is the angle between the axis of CNT i and the direction of the temperature gradient in the network (x-axis) and $\mathrm{Bi}_c = \sigma_c L_T/(k_T A_T)$ is the ratio of the conductance at a single contact to the intrinsic nanotube conductance. The distribution of temperature along CNT i *as a function of coordinate* x can be expressed in the form

$$T_i(x) = T_0 + \nabla T_x x_{C_i} + \left\langle \frac{dT_i}{dx} \right\rangle (x - x_{C_i}) + \delta T_i(x), \quad (3)$$

where T_0 is the averaged sample temperature at $x = 0$, ∇T_x is the temperature gradient imposed in the x direction, $\langle dT_i/dx\rangle$ is equal to ensemble-averaged value of the left hand part in Eq. (2), i.e., $\langle dT_i/dx\rangle = \langle (T_i|_{l_i=L_T} - T_i|_{l_i=0})/(L_T\cos\theta_i)\rangle$ ($\langle\ldots\rangle$ hereinafter denotes averaging over all possible random configurations of CNTs), x_{Ci} is the x coordinate of the center of nanotube i, and $\delta T_i(x)$ accounts for the deviation of the actual temperature from the linear distribution given by the first, second, and third terms. If the density parameter ($\bar{n}_S = n_S L_T^2$ in 2D or $\bar{n}_V = n_V R_T L_T^2$ in 3D samples, where n_S or n_V is the surface or volume number density of nanotubes[17]) is high and aspect ratio of nanotubes, L_T/R_T, is large, then it is reasonable to assume (and numerical simulations support this assumption) that the actual temperature distributions along nanotubes are close to linear ones and, $\delta T_i(x)$ term in Eq. (3) can be neglected. Additionally, for $L_T/R_T \gg 1$, the points of thermal contact on the axes of CNTs i and j become indistinguishable, i.e., $x_{ij} = x_{ji}$, where x_{ij} is the x coordinate of thermal contact between CNTs i and j lying on the axis of CNT i. Then, using Eq. (3) for calculation of $T_j(l_{ji}) - T_i(l_{ij})$ at a large density parameter and $L_T/R_T \gg 1$ and taking into account that for both 2D and 3D samples $\langle\sum_{j=1,\delta_{ij}=1}^{N}(x_{C_j} - x_{C_i})/(L_T\cos\theta_i)(l_{ij}/L_T - 1)\rangle/\langle N_J\rangle = 1/12$ ($\langle N_J\rangle$ is the averaged number of thermal contacts per CNT, $\langle N_J\rangle = (2/\pi)\bar{n}_S$ and $\langle N_J\rangle = \pi\bar{n}_V$ in 2D and 3D samples, respectively[17]), the ensemble-averaged Eq. (2) can be written as

$$\frac{\langle dT_i/dx\rangle}{\nabla T_x} = \frac{\mathrm{Bi}_c\langle N_J\rangle/12}{1 + \mathrm{Bi}_c\langle N_J\rangle/12}. \quad (4)$$

In the framework of the soft-core model,[28,29] the thermal conductivity of both 2D and 3D samples composed of straight nanotubes can be represented in the form[17] $k = k_*\langle N_x\rangle\langle N_J\rangle\langle\Delta T_{(+)}\rangle$, where the coefficient k_*, the averaged number of nanotubes $\langle N_x\rangle$ crossing a unit area perpendicular to the temperature gradient, and $\langle N_J\rangle$ are independent of k_T, whereas the averaged temperature difference at contacts that define the heat flux through a sample cross-section at $x = \mathrm{const}$ (these contacts are located to the right of the cross section), $\langle\Delta T_{(+)}\rangle$, does depend on k_T. Then $k = k^0\langle\Delta T_{(+)}\rangle/\langle\Delta T_{(+)}\rangle^0$, where $\langle\Delta T_{(+)}\rangle^0$ is $\langle\Delta T_{(+)}\rangle$ evaluated at $\mathrm{Bi}_c = 0$. The value of $\langle\Delta T_{(+)}\rangle$ can be expressed as $\langle\Delta T_{(+)}\rangle = \langle\sum_{i=1}^{N}\sum_{j=1}^{N}\delta_{ij(+)}(x)(T_j(x_{ji}) - T_i(x_{ij}))\rangle/\langle\sum_{i=1}^{N}\sum_{j=1}^{N}\delta_{ij(+)}(x)\rangle$, where $\delta_{ij(+)}(x) = 1$ if CNT i intersects the cross section and the point of contact between CNTs i and j is located to the right of the cross section, otherwise $\delta_{ij(+)}(x) = 0$. Using Eq. (3) for the temperatures in the above equation, for a large density parameter and $L_T/R_T \gg 1$, we obtain $\langle\Delta T_{(+)}\rangle/\langle\Delta T_{(+)}\rangle^0 = (1 - \langle dT_i/dx\rangle/\nabla T_x)$ which,

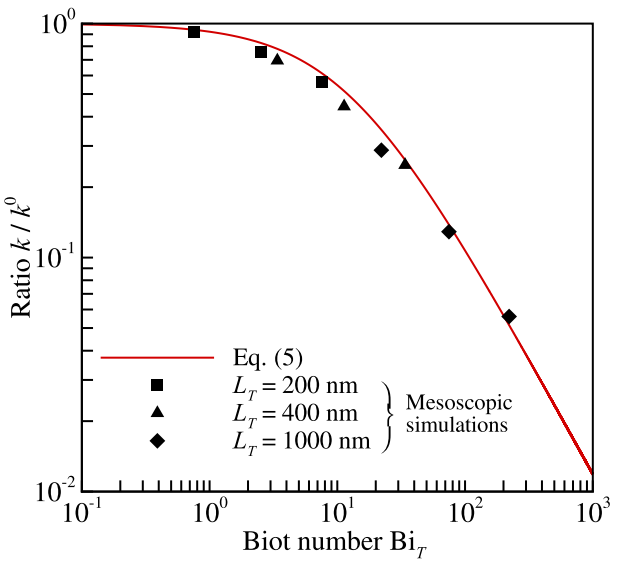

FIG. 3. Ratio k/k^0 vs. Biot number $\mathrm{Bi}_T = \mathrm{Bi}_c\langle N_J\rangle = \sigma_c\langle N_J\rangle L_T/(k_T A_T)$. The curve corresponds to the prediction of Eq. (5). The symbols mark the values of k/k^0 calculated for samples generated in mesoscopic simulations and shown in Fig. 2, with Bi_T calculated based on the average number of thermal contacts $\langle N_J\rangle$ and effective contact conductance σ_c in the network structure (see text).

combined with Eq. (4), yields the final expression for the conductivity of the network material

$$k = \frac{k^0}{1 + \mathrm{Bi}_c\langle N_J\rangle/12} = \frac{k^0}{1 + \mathrm{Bi}_T/12}, \qquad (5)$$

where $\mathrm{Bi}_T = \mathrm{Bi}_c\langle N_J\rangle = \sigma_c\langle N_J\rangle L_T/(k_T A_T)$. Equation (5) shows that the effect of the finite conductivity of individual nanotubes is characterized solely by a new dimensionless parameter Bi_T (curve in Fig. 3). This parameters is equal to the ratio of the total contact conductance $\sigma_c\langle N_J\rangle$ of a nanotube *at all contacts* it has with other CNTs to the intrinsic conductance of the nanotube, $k_T A_T/L_T$. By analogy with the classical interfacial heat transfer problems, Bi_T can be referred to as a Biot number for a nanotube. It is common to assume that the thermal transport processes in a body with a small Biot number are governed by the contact heat transfer, while the body itself can be considered to be isothermal.[30] Since Bi_T characterizes an individual CNT, it can be used as a measure of nonuniform distribution of temperature in an individual nanotube, while a material composed of multiple CNTs can support a substantial temperature gradient regardless of Bi_T. Equation (5) shows that the effect of the intrinsic conductivity of a CNT on the overall conductivity of the CNT material vanishes at $\mathrm{Bi}_T \to 0$, e.g., $k/k^0 > 0.99$ at $\mathrm{Bi}_T < 0.1$. The Biot number Bi_T increases with increasing material density and L_T and it can be fairly large for real materials even if the ratio of the conductance at a single contact to the intrinsic nanotube conductance, Bi_c, is small.

The predictions of Eq. (5) are illustrated in Fig. 4, where the solid curves show the dependence of k on L_T for 3D samples composed of (10,10) CNTs for three values of material density ρ, typical of the CNT films and buckypaper (density is calculated as $\rho = 2\pi R_T L_T m n_\sigma n_V$, where m is the mass of a carbon atom). At small L_T, k practically coincides with k^0 (dashed curves in Fig. 4) and scales quadratically with both ρ and L_T ($k^0 = (\sigma_c/R_T)\pi\bar{n}_V^2/36$ for 3D samples[17]). An increase of L_T at a fixed ρ also increases Bi_T and results in the deviation of k from k^0 as Bi_T approaches and exceeds unity. In the limit of infinitely large Bi_T, the conductivity approaches the asymptotic value of $k^\infty = (1/3)(A_T/(\pi {R_T}^2))k_T\phi$, where $\phi = \pi R_T^2 L_T n_V$ is the volume fraction of nanotubes and, thus, k becomes independent of L_T and linearly proportional to ρ. Thus, Eq. (5) describes a gradual transition between the two limiting scaling laws, $k \propto \rho^2 L_T^2$ at $\mathrm{Bi}_T = 0$ and $k \propto \rho$ at $\mathrm{Bi}_T \to \infty$. Parts of the dependences at $\bar{n}_V < 1$ are shown in Fig. 4 by dash-dotted lines, since the quadratic scaling law for k^0 is derived in Ref. 17 for dense systems and can not be applied close to the percolation threshold.[31]

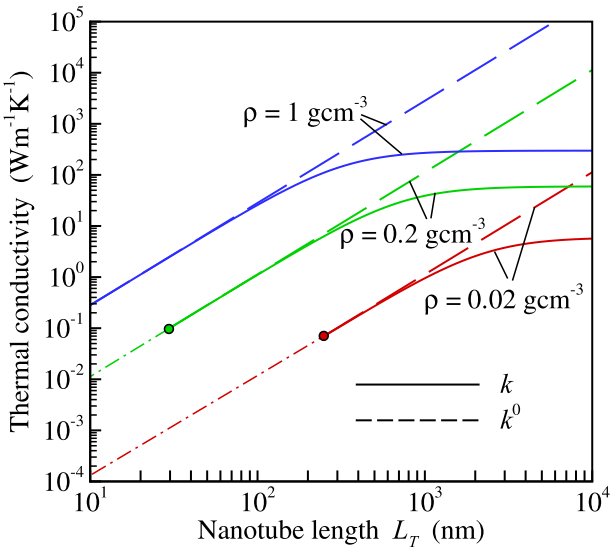

FIG. 4. Dependences of thermal conductivity of 3D samples composed of straight randomly distributed (10,10) CNTs on CNT length L_T calculated with Eq. (5) for $k_T = 2000\,\mathrm{Wm^{-1}K^{-1}}$ (solid curves) and $k_T = \infty$ ($\mathrm{Bi}_T = 0$, dashed curves) at $\sigma_c = 5 \times 10^{-11}\,\mathrm{WK^{-1}}$ and density $\rho = 0.02\,\mathrm{g\,cm^{-3}}$ (red curves), $0.2\,\mathrm{g\,cm^{-3}}$ (green curves), and $1\,\mathrm{g\,cm^{-3}}$ (blue curves). The red and green circles mark nanotube length that corresponds to $\bar{n}_V = 1$ at a given ρ. The values calculated with Eq. (5) at $\bar{n}_V < 1$, when the system is close to the percolation threshold and the quadratic scaling of k^0 with L_T is not valid, are shown by dash-dotted lines.

While Eq. (5) is derived for an idealized system of randomly dispersed straight CNTs, it can also be applied for a semi-quantitative description of continuous networks of bundles characteristic of real CNT materials[22–24] and generated in mesoscopic simulations.[19,20] To apply Eq. (5) to a network of CNT bundles, the values of $\langle N_J\rangle$ and σ_c have to be defined. Taking a sample composed of 1-μm-long (10,10) CNTs with a density of $0.2\,\mathrm{g\,cm^{-3}}$ as an example, $\langle N_J\rangle = 75.1$ can be obtained by counting the number of CNTs that are in thermal contact with each other (are within the cutoff of the "heat transfer" function $\psi(r)$ from each other). This value is almost two times smaller than $\langle N_J\rangle = \pi\bar{n}_V \approx 132$ in a 3D system of straight nanotubes with the same density parameter, $\bar{n}_V \approx 42$, but is still sufficiently large to ensure a substantial deviation of k from k^0. For the contact conductance σ_c, instead of a single value used in the analysis of random arrangements of straight CNTs, the network of bundles exhibits a fairly broad distributions of inter-tube conductance σ_{cij} with a sharp maximum at $\sigma_{\max} = 257\,\mathrm{WK^{-1}}$ (Fig. 5). Distributions of σ_{cij} for samples with $L_T = 200\,\mathrm{nm}$ and

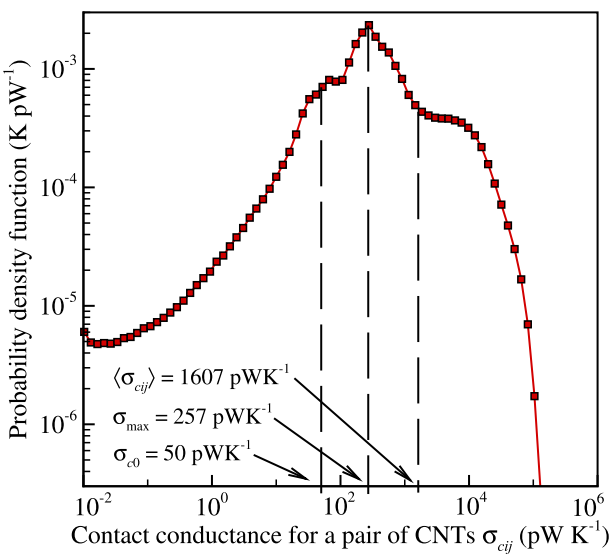

FIG. 5. Probability density function of contact conductance σ_{cij} between a pair of nanotubes in a sample with density of $0.2\,\mathrm{g\,cm^{-3}}$ generated in a mesoscopic simulation and composed of (10,10) CNTs with $L_T = 1\,\mu\mathrm{m}$. $\sigma_{\max} = 257\,\mathrm{pW\,K^{-1}}$ corresponds to the maximum of the distribution, $\langle\sigma_{cij}\rangle = 1607\,\mathrm{pW\,K^{-1}}$ is the value of conductance averaged over all pairs of CNTs that are in thermal contact with each other.

$L_T = 400$ nm have shapes similar to the one shown in Fig. 5 but are slightly shifted towards smaller σ_{cij}. The values of σ_{cij} in a vicinity of $\sigma_{\max}$ are characteristic of CNTs that serve as interconnections between bundles and play an important role in defining the overall conductivity of the material. The thermal contacts with $\sigma_{cij} \gg \sigma_{\max}$ corresponds to CNTs that belong to the same bundle and play a limited role in the heat transfer, since the temperature difference between such CNTs is small (Fig. 1). One can expect that the effective value of σ_c should be between $\sigma_{\max}$ and the average value $\langle \sigma_{cij} \rangle = 1607\,\mathrm{W\,K^{-1}}$. The effective σ_c can also be obtained from the condition of equity of k^0 calculated for the network of bundles and a random 3D system of straight CNTs at the same density. This condition yields $\sigma_c = 886.5\,\mathrm{W\,K^{-1}}$, which is close to $(\sigma_{\max} + \langle \sigma_{cij} \rangle)/2$. With this σ_c and $\langle N_J \rangle = 75.1$, the values of k plotted as a function of Bi_T (diamonds in Fig. 3) are in a good quantitative agreement with prediction of Eq. (5). Similar analysis performed for samples with smaller L_T (triangles and squares in Fig. 3) supports the conclusion that Eq. (5) is suitable for the description of thermal conductivity of continuous networks of CNT bundles.

In summary, mesoscopic simulations predict a strong effect of the intrinsic thermal conductivity of individual CNTs on the overall conductivity of CNT network materials. Theoretical analysis of systems composed of straight randomly dispersed CNTs explains the origin of this effect and yields an equation that describes the dependence of the contribution of k_T to k on the CNT length and material density. The equation is also shown to be suitable for semi-quantitative description of thermal conductivity of continuous networks of bundles characteristic of real CNT films and buckypaper. The theoretical analysis and mesoscopic simulations demonstrate that for a CNT system composed of nanotubes with the characteristic length on the order of micrometers the intrinsic CNT conductivity rather than contact conductance is defining the overall thermal conductivity of the material.

Financial support of this work is provided by the Air Force Office of Scientific Research (Award FA9550-09-1-0245) and the National Science Foundation (Grant CBET-1033919). Computational support is provided by the Oak Ridge Leadership Computing Facility (project MAT009) and the National Science Foundation through the Extreme Science and Engineering Discovery Environment (project TG-DMR110090).

[1]P. Kim, L. Shi, A. Majumdar, and P. L. McEuen, "Thermal transport measurements of individual multiwalled nanotubes," Phys. Rev. Lett. **87**, 215502 (2001).
[2]M. Fujii, X. Zhang, H. Xie, H. Ago, K. Takahashi, T. Ikuta, H. Abe, and T. Shimizu, "Measuring the thermal conductivity of a single carbon nanotube," Phys. Rev. Lett. **95**, 065502 (2005).
[3]Q. Li, C. Liu, X. Wang, and S. Fan, "Measuring the thermal conductivity of individual carbon nanotubes by the Raman shift method," Nanotechnology **20**, 145702 (2009).
[4]A. A. Balandin, "Thermal properties of graphene and nanostructured carbon materials," Nat. Mater. **10**, 569–581 (2011).
[5]E. Pop, D. Mann, Q. Wang, K. Goodson, and H. Dai, "Thermal conductance of an individual single-wall carbon nanotube above room temperature," Nano Lett. **6**, 96–100 (2006).
[6]J. Hone, M. C. Llaguno, N. M. Nemes, A. T. Johnson, J. E. Fischer, D. A. Walters, M. J. Casavant, J. Schmidt, and R. E. Smalley, "Electrical and thermal transport properties of magnetically aligned single wall carbon nanotube films," Appl. Phys. Lett. **77**, 666–668 (2000).
[7]P. Gonnet, Z. Liang, E. S. Choi, R. S. Kadambala, C. Zhang, J. S. Brooks, B. Wang, and L. Kramer, "Thermal conductivity of magnetically aligned carbon nanotube buckypapers and nanocomposites," Curr. Appl. Phys. **6**, 119–122 (2006).
[8]I. Ivanov, A. Puretzky, G. Eres, H. Wang, Z. Pan, H. Cui, R. Jin, J. Howe, and D. B. Geohegan, "Fast and highly anistropic thermal transport through vertically aligned carbon nanotube arrays," Appl. Phys. Lett. **89**, 223110 (2006).
[9]M. E. Itkis, F. Borondics, A. Yu, and R. C. Haddon, "Thermal conductivity measurements of semitransparent single-walled carbon nanotube films by a bolometric technique," Nano Lett. **7**, 900–904 (2007).
[10]R. S. Prasher, X. J. Hu, Y. Chalopin, N. Mingo, K. Lofgreen, S. Volz, F. Cleri, and P. Keblinski, "Turning carbon nanotubes from exceptional heat conductors into insulators," Phys. Rev. Lett. **102**, 105901 (2009).
[11]H. Zhong and J. R. Lukes, "Interfacial thermal resistance between carbon nanotubes: Molecular dynamics simulations and analytical thermal modeling," Phys. Rev. B **74**, 125403 (2006).
[12]S. Maruyama, Y. Igarashi, Y. Taniguchi, and J. Shiomi, "Anistropic heat transfer of single-walled carbon nanotubes," J. Thermal Sci. Technol. **1**, 138–148 (2006).
[13]Y. Chalopin, S. Volz, and N. Mingo, "Upper bound to the thermal conductivity of carbon nanotube pellets," J. Appl. Phys. **105**, 084301 (2009).
[14]Z. Xu and M. J. Buehler, "Nanoengineering heat transfer performance at carbon nanotube interfaces," ACS Nano **3**, 2767–2775 (2009).
[15]V. Varshney, S. S. Patnaik, A. K. Roy, and B. L. Farmer, "Modeling of thermal conductance at transverse CNT-CNT interfaces," J. Phys. Chem. C **114**, 16223–16228 (2010).
[16]J. Yang, S. Waltermire, Y. Chen, A. A. Zinn, T. T. Xu, and D. Li, "Contact thermal resistance between individual multiwall carbon nanotubes," Appl. Phys. Lett. **96**, 023109 (2010).
[17]A. N. Volkov and L. V. Zhigilei, "Scaling laws and mesoscopic modeling of thermal conductivity in carbon nanotube materials," Phys. Rev. Lett. **104**, 215902 (2010).
[18]P. Keblinski and F. Cleri, "Contact resistance in percolating networks," Phys. Rev. B **69**, 184201 (2004).
[19]A. N. Volkov and L. V. Zhigilei, "Mesoscopic interaction potential for carbon nanotubes of arbitrary length and orientation," J. Phys. Chem. C **114**, 5513–5531 (2010).
[20]A. N. Volkov and L. V. Zhigilei, "Structural stability of carbon nanotube films: The role of bending buckling," ACS Nano **4**, 6187–6195 (2010).
[21]L. V. Zhigilei, C. Wei, and D. Srivastava, "Mesoscopic model for dynamic simulations of carbon nanotubes," Phys. Rev. B **71**, 165417 (2005).
[22]A. G. Rinzler, J. Liu, H. Dai, P. Nikolaev, C. B. Huffman, F. J. Rodríguez-Macías, P. J. Boul, A. H. Lu, D. Heymann, D. T. Colbert, R. S. Lee, J. E. Fischer, A. M. Rao, P. C. Eklund, and R. E. Smalley, "Large-scale purification of single-wall carbon nanotubes: Process, product, and characterization," Appl. Phys. A: Mater. Sci. Process **67**, 29–37 (1998).
[23]F. Hennrich, S. Lebedkin, S. Malik, J. Tracy, M. Barczewski, H. Rösner, and M. Kappes, "Preparation, characterization and applications of free-standing single walled carbon nanotube thin films," Phys. Chem. Chem. Phys. **4**, 2273–2277 (2002).
[24]S. Wang, Z. Liang, B. Wang, and C. Zhang, "High-strength and multifunctional macroscopic fabric of single-walled carbon nanotubes," Adv. Mater. **19**, 1257–1261 (2007).
[25]J. Che, T. Çağın, and W. A. Goddard III, "Thermal conductivity of carbon nanotubes," Nanotechnology **11**, 65–69 (2000).
[26]S. Maruyama, "A molecular dynamics simulation of heat conduction in finite length SWNTs," Physica B **323**, 193–195 (2002).
[27]G. Zhang and B. Li, "Thermal conductivity of nanotubes revisited: Effects of chirality, isotope impurity, tube length, and temperature," J. Chem. Phys. **123**, 114714 (2005).
[28]I. Balberg, C. H. Anderson, S. Alexander, and N. Wagner, "Excluded volume and its relation to the onset of percolation," Phys. Rev. B **30**, 3933–3943 (1984).
[29]L. Berhan and A. M. Sastry, "Modeling percolation in high-aspect-ratio fiber systems. I. Soft-core versus hard-code models," Phys. Rev. E **75**, 041120 (2007).
[30]F. Kreith and M. S. Bohn, *Principles of Heat Transfer* (6th ed., Brooks/Cole Pub., Pacific Grove, 2001).
[31]The percolation threshold in a 3D random system of soft-core spherocylinders depends on R_T/L_T, e.g., percolation occurs at $\bar{n}_V = 0.38$ ($\langle N_J \rangle = 1.19$) for $R_T/L_T = 0.003$ and at smaller $\bar{n}_V$ for smaller R_T/L_T [Z. Néda, R. Florian, and Y. Brechet, "Reconsideration of continuum percolation of isotropically oriented sticks in three dimensions," Phys. Rev. E **59**, 3717–3719 (1999)].